



Evaluating capacitive wetness sensors for measuring deposition in electrostatically charged spraying operations

Luke Longworth^a, Scott Post^b, Mark Jermy^{a,*}, Hugh Hendrickson^a, Jamie Steel^a, Ethan Cannon^a, Jack Gleadow^a, Simon Brown^a

^a University of Canterbury, Private Bag 4800, Christchurch 8140, New Zealand

^b Lincoln Agritech Limited, Lincoln University, Engineering Drive, Lincoln 7674, New Zealand

ARTICLE INFO

Keywords:

Electrostatic spraying
Capacitive wetness sensor
Surface moisture sensor
Calibration
Water sensitive papers

ABSTRACT

Standard methods for measuring pesticide deposition include water sensitive paper and fibre (paper or cord) collectors, which require time consuming manual steps to gather, process and interpret results. Measurement of pesticide deposition is important in evaluating the efficacy of a spray, which affects the total crop yield. A lack of knowledge about spray quality often results in the need to spray to excess, which can contaminate the soil and damage neighbouring ecosystems and the atmosphere. The suitability of PHYTOS 31 capacitive leaf wetness sensors (Meter Group, Pullman, WA, USA) for spray sensing applications was analysed. The best fit calibration function for droplets of $\sim 1 \mu\text{L}$ volume was linear ($R^2 = 0.985$). The best fit calibration function for drops $> 10 \mu\text{L}$ was a weighted sum of a linear and power function ($R^2 = 0.984$). Thus, the calibration function should be chosen according to the anticipated size of droplet. The PHYTOS 31 sensors and water sensitive papers were used in a field test, comparing electrostatically charged and uncharged sprays. Both measurement techniques show that charged spray is more effective in covering parts of the plants which do not have a direct line of sight to the nozzle. The techniques disagree on quantitative coverage measurement, with the water sensitive papers reporting areal coverage two to four times higher than the capacitive sensors. High-speed video observations show that this is due to contraction (de-wetting) of the drop on the capacitive sensors. The surface of the capacitive sensors is more hydrophobic than the papers. The hydrophobicity of the capacitive sensors appears to be a better match to plant leaves than that of the papers. Capacitive sensors are a suitable measurement tool for evaluating liquid coverage in the field, but further calibration is necessary to be confident in the quantitative data.

1. Introduction

The spraying of pesticides is an essential part of commercial growing operations around the world. In 2017, 4.1 billion kg of pesticides were used worldwide (UN Food and Agriculture Organization, 2020). Between 2010 and 2014 the mean annual pesticide use was 2.78 kg/ha on a farm level, or 645 mg/kg of crop (Zhang, 2018). There are economic, health and environmental drivers to improve the processes of pesticide spraying (Kishi et al., 1995; Law, 2001; Marlborough District Council, 2015; World Health Organisation, 2018). Pesticides serve a number of functions, including reducing the proportion of plants that die due to infection, or due to insects or other animals eating them, as well as by reducing the competition in the soil due to weed growth (Nazarko et al., 2002). In many cases, it is not commercially viable to grow crops

without spraying.

In traditional spraying procedures, as much as 50–78% of spray will be wasted, either due to entirely missing the plant or by dripping off the plant after contact is made (Fox et al., 1998; Law, 2001), with this pesticide spray being deposited onto the soil or being caught in wind (McEvoy, 1998). Furthermore, of the 30–40% of spray that lands on the surface of the plant, the spatial distribution is skewed to the top surfaces of leaves, and often to the outer layers of leafy canopies (Ferguson et al., 2016). Due to the desirability of total coverage with contact chemicals, most spraying operations spray until there is visible run-off from the plant (Australian Wine Research Institute, 2010). This usually provides adequate coverage, but is excessive, and exacerbates waste and pollution. This method is adopted due to the difficulty of conducting thorough tests to verify good coverage.

* Corresponding author.

E-mail address: mark.jermy@canterbury.ac.nz (M. Jermy).

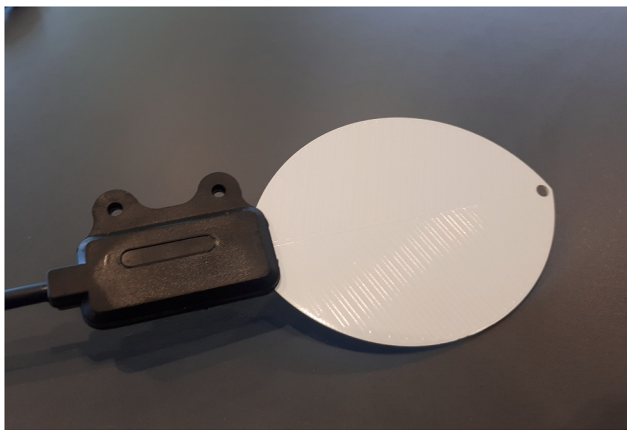


Fig. 1. PHYTOS 31 capacitive wetness sensor.

Capacitive wetness sensors have been used for estimating spray coverage, detecting rain, and detecting moisture content in stored crops. (Clark, 2018) used a Decagon capacitive leaf wetness sensor (LWS) as an alert for rainfall. In this case, the sensor was used as a binary on/off and was not calibrated to area or mass. The Decagon LWS is structurally identical to the LWS marketed by Meter as the PHYTOS 31 (used in this study) and by Campbell Scientific. (Camuffo et al., 2018) used LWS to measure humidity and condensation in buildings, but did not seek liquid water coverage measurements. (Kawahara et al., 2012) constructed a novel LWS using inkjet printing with silver nanoparticle ink, and (Hornero et al., 2017) developed a sensor very similar to the PHYTOS 31 and compared the two, finding that the different sensors differed particularly in terms of drying time. (Kesterson et al., 2015) developed a similar sensor and tested the response to typical agricultural spray nozzles. (Ehlert et al., 2019) performed a 3 year outdoor test on six different commercially available capacitive or resistive sensors, finding the Decagon model to be the most stable, though they did comment that it (and two other sensors) reported moisture in some periods where it was not visible on a timelapse camera in the area.

(Acharya et al., 2017) used LWS underneath the leaf litter on a forest floor to measure moisture levels, and when calibrating the sensor output to gravimetrically measured percent water content they found a quadratic function to be suitable. (Meter Group Inc.) produced a calibration between sensor output and mass per unit area and fitted an exponential function to it. (Wang et al., 2019) calibrated the PHYTOS sensors and found a linear relationship between mass and sensor output, with non-ionic solutions (pure water and non-ionic herbicides) having the same slope and ionic solutions having a different slope. (Foque et al., 2018) calibrated a Delta OHM HD3901 sensor, which is similar to the PHYTOS 31. Single droplets were detectable down to a threshold of 2 L/ha. They also performed spray tests on these sensors, using water sensitive papers to measure areal coverage and comparing this to sensor output. In these tests, they found a linear correlation between sensor

output and spray areal application rate, with signal depending on droplet size (attributed to contact angle and coalescence). Similarly, Hornero et al. attributed a spike and decay time-pattern in sensor signal to coalescence of droplets on the surface, reducing coverage slightly after the droplets were deposited.

Taking a different approach, Wen et al. (Wen et al., 2019) developed a spray coverage sensing system that is not capacitive, but uses a fluorescent dye in the spray, deposited onto kraft paper strips which are later analyzed in a spectrometer. This circumvented some of the handling issues of water sensitive papers and has low ongoing costs.

No publication to date has reported a calibration of a capacitive LWS that compares sensor output to areal coverage over the full range from dry to fully covered. This study aims to fill this gap by producing a calibration of the PHYTOS 31 sensors that covers a wider range of sensor output values and to describe them in the context of percent sensor output. It also compares differences in sensor behaviour for large droplets and fine sprays. Finally, the areal coverage of the sensor is measured photographically rather than inferred from nearby water sensitive papers, finding that droplet spreading and retraction behaviour differs on the two different sensor surfaces.

2. Sensor calibration

2.1. Sensors

PHYTOS 31 (Meter Group, Pullman, WA, USA) capacitive wetness sensors (Fig. 1) were the subject of this investigation. These have interdigitated conductive tracks distributed over the surface, encapsulated with a polymer coating. The capacitance of the interdigitated electrodes is directly influenced by the dielectric constant of material occupying the space near the surface of the sensor, which is modified by the presence of water. On-board signal conditioning produces a DC voltage output. This was read with either a 14 bit National Instruments (Austin, TX, USA) analogue to digital converter (ADC; NI USB-6009, 150 Hz, 5 V excitation) connected to a PC running National Instruments LabView, or to a 16-bit ADC unit (ADS1115, Texas Instruments, Dallas, Texas, USA) connected to an Arduino Nano (5 V excitation; Arduino AG, Turin, Italy). Allowing for the difference in resolution, these gave similar mean and noise levels. Such sensors provide real-time information and may find use in monitoring of spray operations.

2.2. Calibration versus areal coverage

Preliminary tests with water films of different thicknesses and with different droplet distributions (i.e. one large drop compared to several small drops with the same total mass) indicated that the sensor signal was sensitive to both areal coverage (fraction of the sensitive surface in contact with liquid water) and volumetric coverage (volume of the bodies of water in contact with the sensitive surface), with areal coverage dominating the signal. This was expected as the capacitance is



Fig. 2. Example of image processing typical during the sensor calibration.

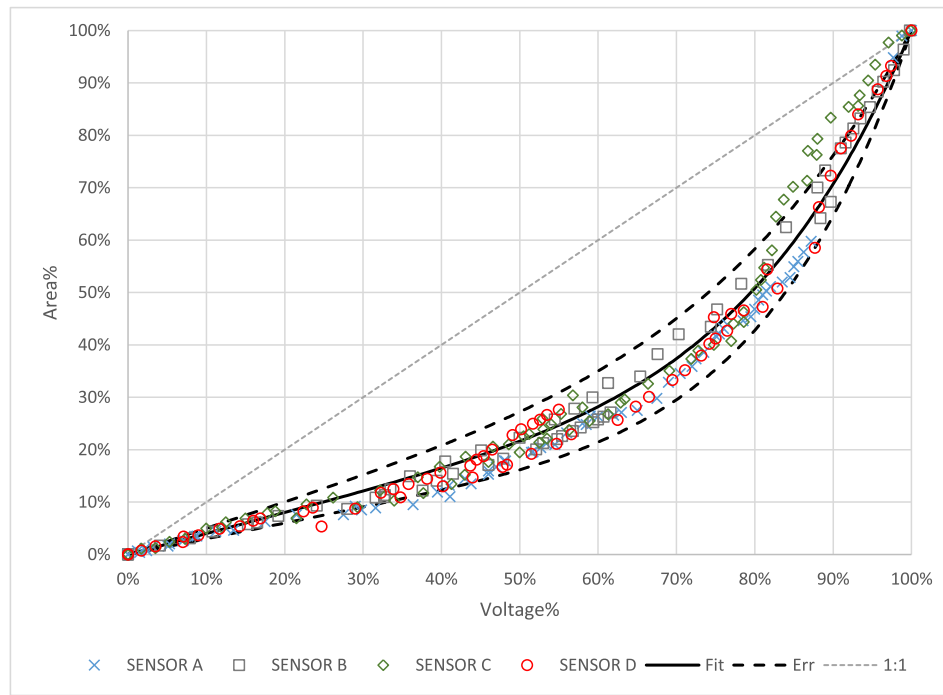


Fig. 3. Calibration data compared to a 1:1 relationship (Eq. (4)). The curve labelled “Fit” follows Eq. (3).

sensitive only to dielectric materials in close proximity to the electrodes. Thus, for the remainder of the study, areal coverage was considered rather than volumetric coverage or mass. To obtain a calibration function, a series of droplets of red water (dyed with Pillar Box Red food colouring diluted with water to 10% by volume, Queen Fine Foods Pty Ltd, Australia) were placed onto the surface of the sensor with a pipette, producing droplets typically of volume $> 10 \mu\text{L}$ and diameter (after spreading on the sensor surface) 5–10 mm. The sensor DC voltage was recorded while the sensor surface was simultaneously imaged with a digital camera at a resolution of 1280×720 pixels (Logitech, Lausanne, Switzerland) from which actual areal coverage was measured. This led to two sets of data, a sensor DC output level and one image, for each drop added to the sensor. Tests were done on four separate sensors to establish whether any relationships found were indicative of the sensors in general, rather than to one particular sensor.

Images of the sensor surface were processed using MATLAB (Mathworks, Natick, Massachusetts, USA). Images were separated into their red, green and blue components, and a greyscale image was produced by subtracting the brightness of the green and blue components from the red component. This converted all pixels that were not predominantly red to a very dark grey or black. The images were then binarised using the threshold chosen by the MATLAB *imbinarize* function (implementing Otsu’s method), and then the total number of white pixels were counted. An example of this processing can be seen in Fig. 2. By comparing the number of pixels of red to the number of pixels occupied by the whole sensor, a percentage areal coverage can be calculated using Eq. (1). The total sensor area was calculated either using a fully covered sensor (where possible), or by using a simple *rgb2gray* conversion and binarising with an appropriate threshold.

$$AC_{image} = \text{ArealCoverage}_{image} = \frac{\# \text{blackpixels}}{\# \text{pixels}} \quad (1)$$

The DC voltage output from the sensor’s on-board signal conditioning unit was converted into a fraction by dividing by the range (Eq. (2)):

$$AC_{voltage} = \text{ArealCoverage}_{voltage} = \frac{\text{Signal} - \text{Min.Signal}}{\text{Max.Signal} - \text{Min.Signal}} \quad (2)$$

The minimum and maximum signals are the lowest and highest

signals recorded by the ADC respectively. These were found using the *MIN()* and *MAX()* functions in Microsoft Excel. This guarantees that the 100% and 0% readings from both measurement sources were the same. AC_{image} and $AC_{voltage}$ were plotted so that a calibration function relating the two could be established (Fig. 3).

The indicated signal is monotonic, but not linear, with the areal coverage measured in the image, and calibration is required. Various fits were tested, including bi-linear, quadratic, exponential, and power fits. Whilst the R^2 value for many of them was reasonably high, the error on particular sections of the curve was undesirable. For example, bi-linear fits had R^2 values close to 0.95, but on the range of 25% to 80% the data suited any of the curve fits better. Contrary to this, a curve fit usually suited the centre of the data well but was inaccurate in the early 20%, which is where much of the data in agricultural spray tests lies. Ultimately, a weighted sum of a linear fit and a power fit was used, the form of which can be seen in Eq. (3). It was required that the function fit be non-negative, non-decreasing and concave up throughout the interval $[0, 1]$ which adds the restrictions of $0 < a < 1$ and $b > 1$ (see Section Appendix for details). MATLAB was used to find the (a, b) pair that maximized R^2 for each dataset. The final (a, b) pair had the value of a adjusted to more closely follow the lower linear section, and b was optimised accordingly. The optimised pair was $(a = 0.4, b = 5.2)$ produces a coefficient of variation (R^2) of 0.984.

$$AC_{image} = a * AC_{voltage} + (1 - a) * (AC_{voltage})^b \quad (3)$$

The calibration test featured only large droplets which are not typical of agricultural sprays, and assumed that full coverage should be interpreted as the value read when the sensor is fully covered with a thin layer of liquid. In a real spraying operation, run-off will prevent this condition from being met. A second calibration test was carried out using a hand-pumped household aerosol spray bottle, producing droplets of a variety of sizes, of order $1 \mu\text{L}$ and 0.5–2 mm in diameter when spread on the sensor surface.

To capture the small deposited droplets, higher resolution images were needed. The rear-facing 16MP camera on an LG V30 + mobile phone was used to capture images at 4656×3492 pixels, with 72 pixels per inch. To account for changes in viewing angle, the total area of the

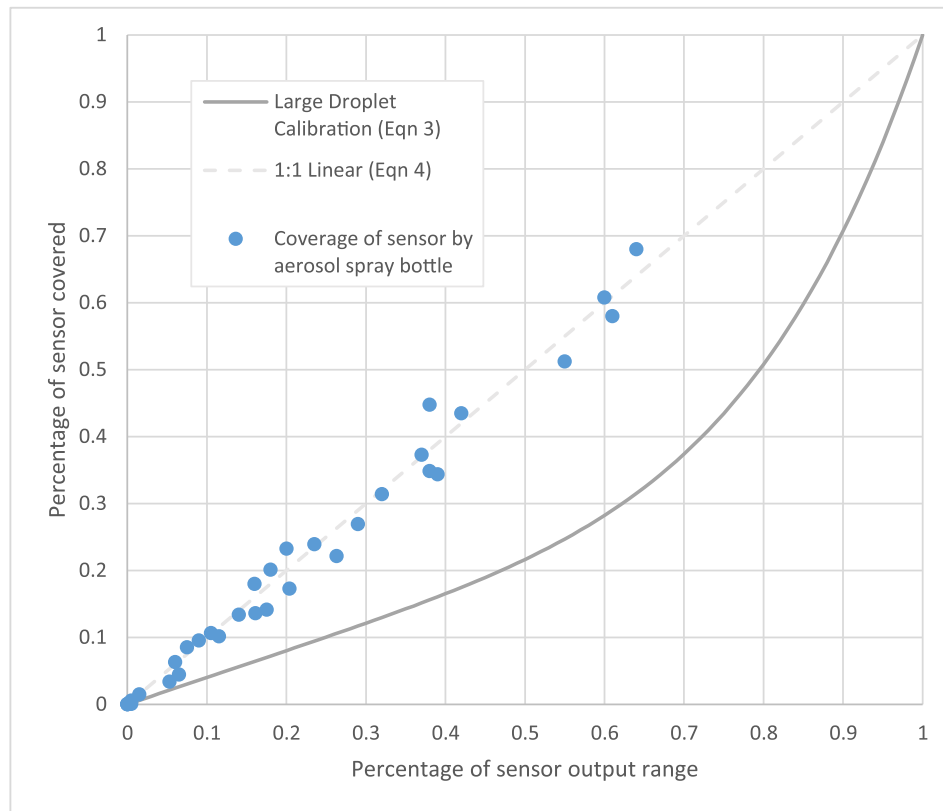


Fig. 4. Comparison of aerosol spray bottle data to calibration function.

sensor was calculated for each image. The smallest droplets were not detected by the camera, and the smallest that were detected were not recognised by the MATLAB post-processing routine, so each of the visual coverage values will be underestimates of the true value. As these are the smallest droplets, the error is expected to be small. Water sensitive papers have the same fault (small drops are omitted when the papers are scanned).

The comparison between this spray bottle data and the calibration functions can be seen in Fig. 4. The calibration function of Eq. (4), obtained from drops deposited with the pipette, underestimates the coverage applied by the spray bottle. This may be due to:

- Depth of the deposited drops. The pipette deposits deeper drops than the spray bottle.
- Distance of the deposited drops from the conductors of the interdigitated capacitor (the parallel lines visible in Fig. 1). The pipette deposits drops which straddle more than one conductor. The spray bottle drops do not, unless they merge with neighbouring drops. Drops which are distant from a conductor will not change the capacitance as much as drops deposited over a conductor.

With the small drops from the spray bottle, the sensor signal shows a 1:1 linear relationship where the proportion of total sensor output range maps directly to the proportion of the sensor area covered by liquid. The resulting linear calibration function (Eq. (4)) has an R^2 of 0.9845, comparable to that achieved for large drops by the calibration function in Eq. (3).

$$AC_{image} = AC_{voltage} \quad (4)$$

2.3. Error bounds

Additional functions were defined to encompass the bounds of uncertainty of the large droplet calibration (Eq. (3)). These functions were chosen manually using different (a, b) pairs chosen to fit the range of data produced by the several pipette calibration runs represented in Fig. 3. Specifically, the upper error used (0.5, 4.5) and the lower error used (0.3, 5.9). These bounds encompass most points, with 91% of points falling below the upper error and 95.5% of points falling above the lower error. The specific a and b values were chosen such that Eq. (5) is true. A similar process was applied to the small droplet calibration

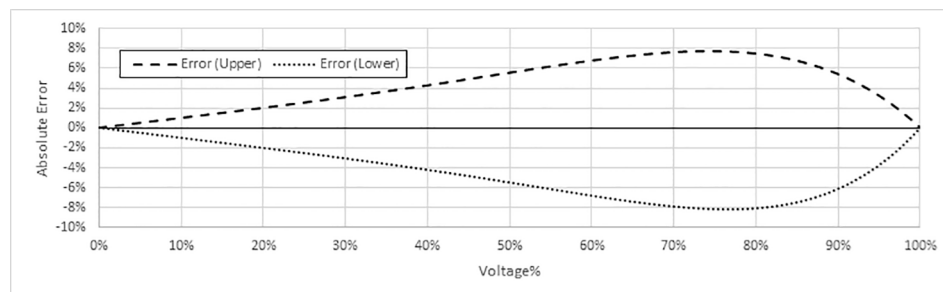


Fig. 5. Error function for Eq. (3).

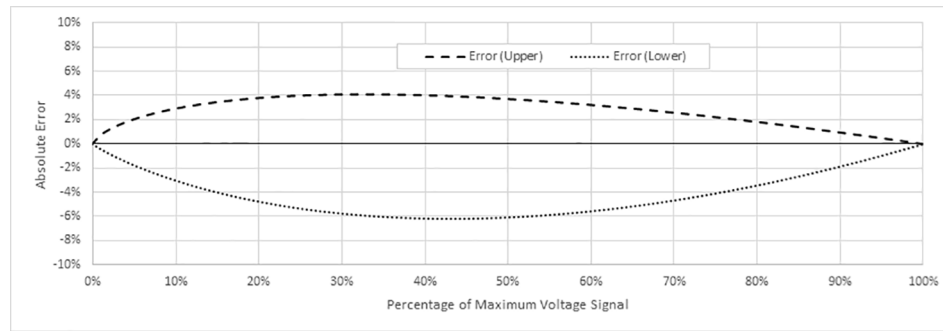


Fig. 6. Error function for Eq. (4).

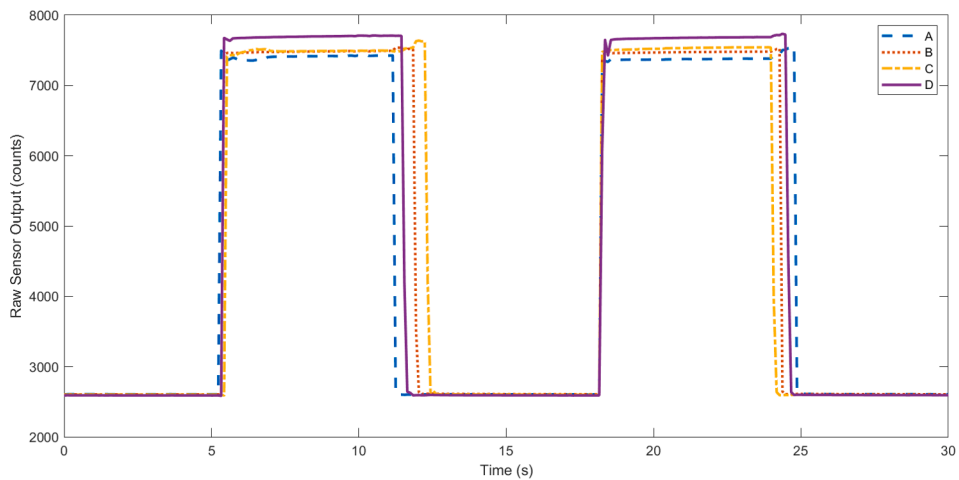


Fig. 7. Stability test for all four wetness sensors; full range.

Table 1

Quantification of stability at maximum and minimum. StD is standard deviation.

	1st Minimum		1st Maximum		2nd Minimum		2nd Maximum		3rd Minimum	
	Mean	StD								
A	2608.5	0.5	7419.9	2.9	2606.6	0.5	7377.4	2.5	2608.5	0.5
B	2606.0	0.3	7486.5	2.9	2608.8	0.7	7477.4	1.5	2607.3	0.5
C	2603.2	0.4	7489.3	3.5	2602.7	0.7	7539.0	1.9	2596.5	0.5
D	2592.2	0.5	7702.0	3.0	2592.5	0.5	7682.9	1.9	2595.5	0.6

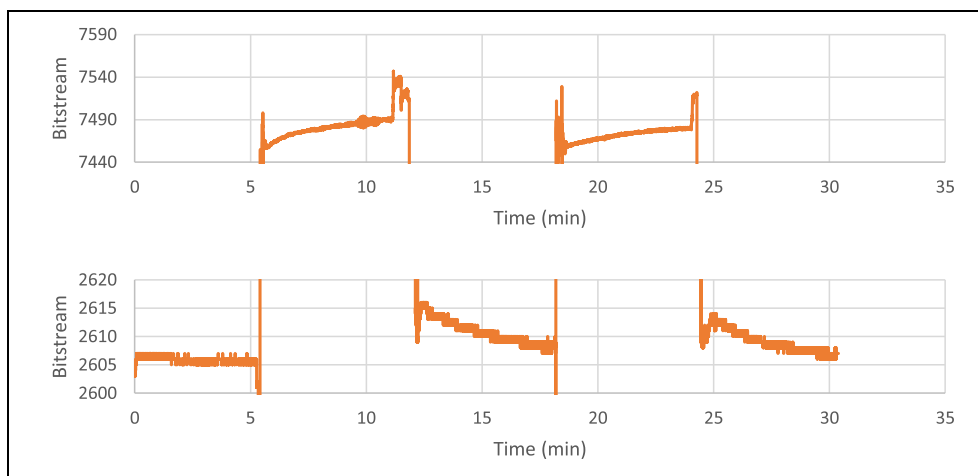


Fig. 8. Stability test for sensor B; split axes with variable vertical axis scaling.



Fig. 9. Sensor layout for trunk-wraparound sensor comparison test. (a) Shows the setup without papers attached and (b) includes papers.

(Eq. (4)), with this error function being asymmetrical but only relying on one variable, c . These error bounds are seen in Eq. (6). Figs. 5 and 6 visualise the error, with the former showing that the error is small for low input values but approaches an output deviation of 8% around an input of 0.75, and the latter showing lower overall error but more asymmetric curves. The error curves for Eq. (3) are included in Fig. 3.

$$AC_{image} = (0.4 \pm 0.1)AC_{voltage} + (0.6 \mp 0.1)(AC_{voltage})^{5.2 \pm 0.7} \quad (5)$$

$$AC_{image} = 0.5AC_{voltage}(1 + AC_{voltage}^c) \text{ with } c \in (-0.2, 0.4) \quad (6)$$

2.4. Repeatability

To quantify the repeatability, all four sensors (labelled A to D) were simultaneously submerged, removed and dried with a paper towel, and left in the air. This was done twice, with each period of immersion and airing lasting approximately 5 min. The results can be seen in Fig. 7. The four sensors A to D were taken out and dried in turn, hence the slightly different timing of the falling edge.

The variation in sensor maximum and minimum values for each sensor is quantified in Table 1, and an example of the maxima and minima for sensor B can be seen in Fig. 8. The variation was calculated by evaluating the mean and standard deviation over the most stable sections of each segment (roughly the last quarter of the period). The maxima/minima visualisation in Fig. 8 is made by cropping the vertical axis to values that encompass the whole of the stable section, but little of the rising or falling portions.

Some observations from this include:

- After drying with a cloth, the signal still gradually decreases. This is likely due to continued evaporation on the surface of the sensor. Whilst the signal appears to be approaching the original zero point, it seems to take longer than 5 min to reach this. However, in 5 min it approaches the original zero to within 0.2% (10 bits out of a total range of ~ 5000 bits).
- When submerged, there is a gradual upwards trend over time. This effect is reminiscent of the gradual decrease mentioned in the previous point, and may be attributed to the presence of small bubbles on the surface of the sensor, leaving the surface of the sensor over time. Again, it appears this process lasts >5 min before the signal stabilizes.
- There are some transient effects whilst drying with a cloth, wherein there is a small minimum before the long-term drying process takes place. This can be seen around 12 min and 24 min in the bottom of Fig. 7, and it is unclear what this is caused by. One possible explanation is that this comes from the pressure of the cloth causing the surface to deform slightly.
- As one sensor is taken from, or placed in, the water, the other sensors experience a noticeable spike in their signal. This can be seen in the

top of Fig. 8 at around 12 min and 24 min, and is also noticeable in all four sensors in Fig. 7. This may be due to crosstalk between the sensors, between the cables or in the ADC, due to the motion of the cable through Earth's magnetic field, or some other cause.

- The high signal varies over a range of close to 50 bits, which is fivefold bigger than the range of the low signal.

2.5. Back side sensitivity

The sensor's sensitive side was placed on the surface of a pool of water such that the entire sensitive side was covered but the back was completely dry. The sensor was then removed, dried, turned over, and placed back in the pool, such that this time only the back side was covered. When the non-sensitive side was covered, a stable result equalling approximately 2.5% that of the sensitive side was obtained. This suggests that the error of the sensor due to deposition on the back side is minimal, and acceptable in most agricultural operations.

3. Comparison to water sensitive papers

3.1. Vine trunk spray wrap-around test

A set of measurements were made in the vineyard owned and managed by Lincoln University (Lincoln, South Island, New Zealand). Of interest was the wrap-around effect, in which spray travels to the far side (obscured surface) of an object. The wetness sensors were attached the base of a vine trunk, one in the front, one on the side, and one on the back. An image of this arrangement can be seen in Fig. 9. A modified BP1 electrostatic spraying nozzle (Electrostatic Spraying Systems, Watkinsville, GA, USA) was used to spray the sensors for 10 s at a time, with half of the trials having charged spray (with the electrode at roughly 1 kV) and the other half having uncharged spray. From phase-Doppler measurements at similar operating conditions we estimate the Sauter Mean Diameter to be 50–60 μm (Longworth, 2020). The sensors were dried between trials. Following this, a set of tests were performed that were identical to the previous tests except that the sensors were not switched on and instead had a water sensitive paper pegged to them. After each trial, the water sensitive papers were placed in individual, labelled, dry, plastic zip lock bags. The papers were not used on the front sensor after the first test because they saturated completely in the 10 s test.

The intention of this test was to verify that the increase in deposition based on charging the spray was consistent between the two sensing methods. Thus, the capacitive sensor data was processed using Eq. (6) to produce an estimated areal coverage. The water sensitive papers were scanned at 600 dpi, the images cropped to size, and then evaluated with an adjusted version of the MATLAB script used earlier to calibrate the capacitive sensors. The adjusted script separated the yellow, blue and white by first taking the unweighted average of the R, G and B channels of the picture and binarising this (to find the total area of the paper

Table 2

Example of processing steps for the wetted papers.

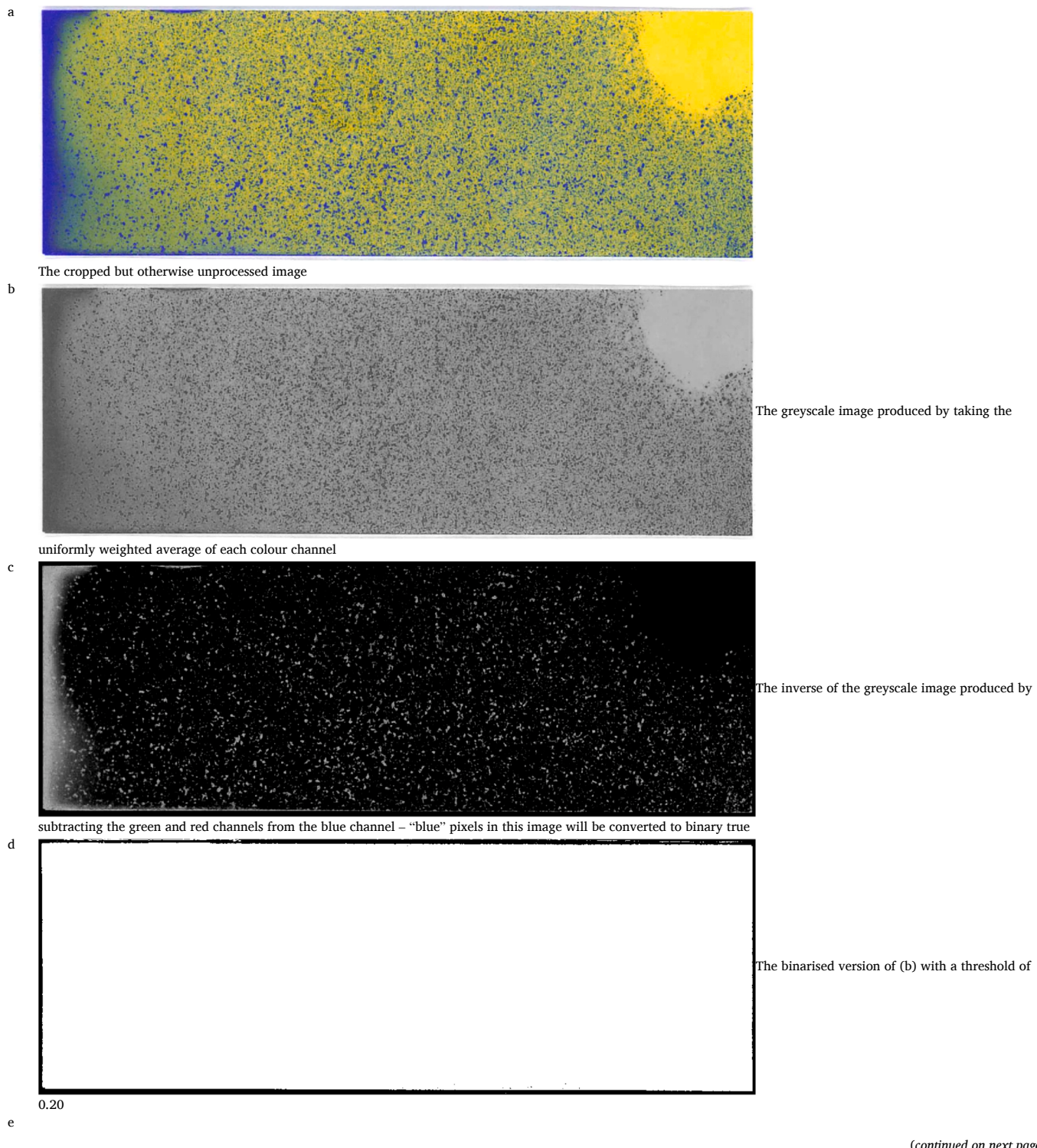
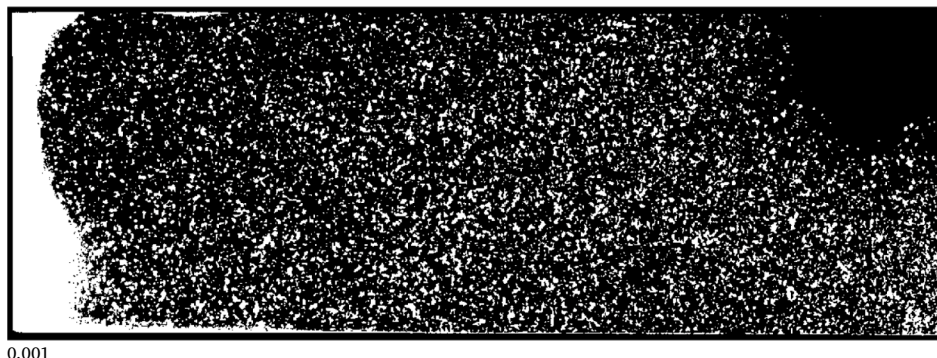


Table 2 (continued)

The binarised version of (c) with a threshold of

0.001

Table 3
Coverage values for the two different sensing methods.

	1	Capacitive sensor			Water sensitive paper	
		Front	Side	Back	Side	Back
Uncharged	2	10.5%	1.2%	0.1%	N/A	0.8%
	3	18.2%	2.2%	0.1%	1.8%	0.0%
	3	20.4%	1.0%	0.2%	1.2%	0.0%
Charged	1	22.7%	4.3%	0.8%	N/A	2.7%
	2	16.2%	3.3%	2.3%	13.9%	2.1%
	3	16.2%	3.2%	1.2%	21.4%	0.6%

Table 4
Coverage increase due to electrostatic spraying.

	1	Capacitive sensor			Water sensitive paper	
		Front	Side	Back	Side	Back
Min	0.79	1.46	3.08	7.67	0.76	
Average	1.16	2.47	8.54	11.72	6.37	
Max	2.17	4.31	19.01	17.83	1254.87	

itself), and then creating a new image that subtracted the red and green channels from the image before binarising this image too (in the same way that the previous analysis subtracted green and blue). The first binarisation used a threshold of 0.20 which was selected manually as the value that seemed to visually represent the area the best. The second binarisation used a forced manual minimum threshold of 0.001 because any pixel that had a small blue level would already be set to 0 because of overflow in the subtraction. Examples of steps in the image processing sequence are shown in **Table 2**. The coverage was calculated as the number of blue pixels divided by the total number of pixels in the paper (i.e. the number of pixels in the cropped image excluding the white boundary). The results are shown in **Tables 3** and **4**.

Table 4 is an amalgamation of these results; it shows the proportional increase in coverage when the spray is charged. The “average” row shows the mean of all charged trials divided by the mean of all uncharged trials. The “min” and “max” rows respectively show the smallest and largest value that could be calculated with the data. Because each average value is >1 , this gives the indication that charging the spray always increases the amount of liquid on the sensor or paper, though the amount of increase varies. Additionally, the range of min to max varies greatly between tests.

To better understand the differences between the two sensing methods, high speed images of droplets striking the sensor surfaces were obtained. A PHYTOS 31 sensor and a water sensitive paper were attached to a vertical surface and sprayed with a handheld aerosol spray bottle filled with red-dyed water (the same as detailed in Section 2.2). The sensors were illuminated with a 20,000 lm white LED light and imaged with a Photron SA5 camera (12 bit, 1024×1024 pixels,

Photron, Toyko, Japan) at 2500fps fitted with a 50 mm Nikkor photographic lens. A sequence of images is shown in **Fig. 10**. The gamma correction was adjusted to obtain good contrast, and no other post-processing was done.

On the PHYTOS 31 sensor surface, the larger droplets were observed to spread and then retract (de-wet) to occupy a smaller area on the sensor. On the water sensitive paper, this retraction was not apparent.

4. Discussion

The PHYTOS 31 capacitive sensors are characterised by the following qualities:

- Rise time of <0.2 s, with the last 1% of the total signal taking >5 min to settle. It is hypothesised that this last 1% change in signal is due to either small amounts of water evaporating over time, or by bubbles in the water near the surface of the sensor gradually dissolving. The local minima observed before the slow drying process were unexplained, though it has been suggested that it may be due to the pressure of the drying cloth.
- Variation in the maximum signal may be up to 30 bits (0.6% of maximum bit range), but the minimum signal has a variation of no >10 bits (0.2% of maximum range). Additional variations in the maximum signal were observed when nearby sensors were moved out of the water, producing a sudden, drastic change in signal. This is attributed to crosstalk between the adjacent wires.
- Linear relationship between areal coverage and voltage signal for small drops.
- For large drops the linear relationship overestimates areal coverage, and a better calibration function is a weighted sum of a linear and a power function, giving an R^2 value of 0.984.

The capacitive sensors give results that are qualitatively sensible. Adding more liquid to the surface produces a signal that increases monotonically, and the signal received from a sensor when dry and when fully submerged are consistent between tests. The calibration tests with the red dye were also consistent and repeatable, with each individual sensor producing results that, whilst not identical, were very similar to one another such that a single calibration function is suitable for all sensors within one spraying type. However, the calibration curve varies for different drop sizes (pipette $> 10 \mu\text{L}$ or aerosol spray bottle $\sim 1 \mu\text{L}$). This may be due to the larger drops having greater depth, hence a greater effect on capacitance, for the same areal coverage. A similar drop size effect was noted, with much larger drops (Kesterson et al., 2015).

Both measurement techniques showed that the deposition on the sides and back of the trunk was increased when the spray was charged, the specific amounts and proportional increases differed. In particular, the measurements on the side of the trunk were significantly larger for the water sensitive papers (13–21%) than they were for the sensors

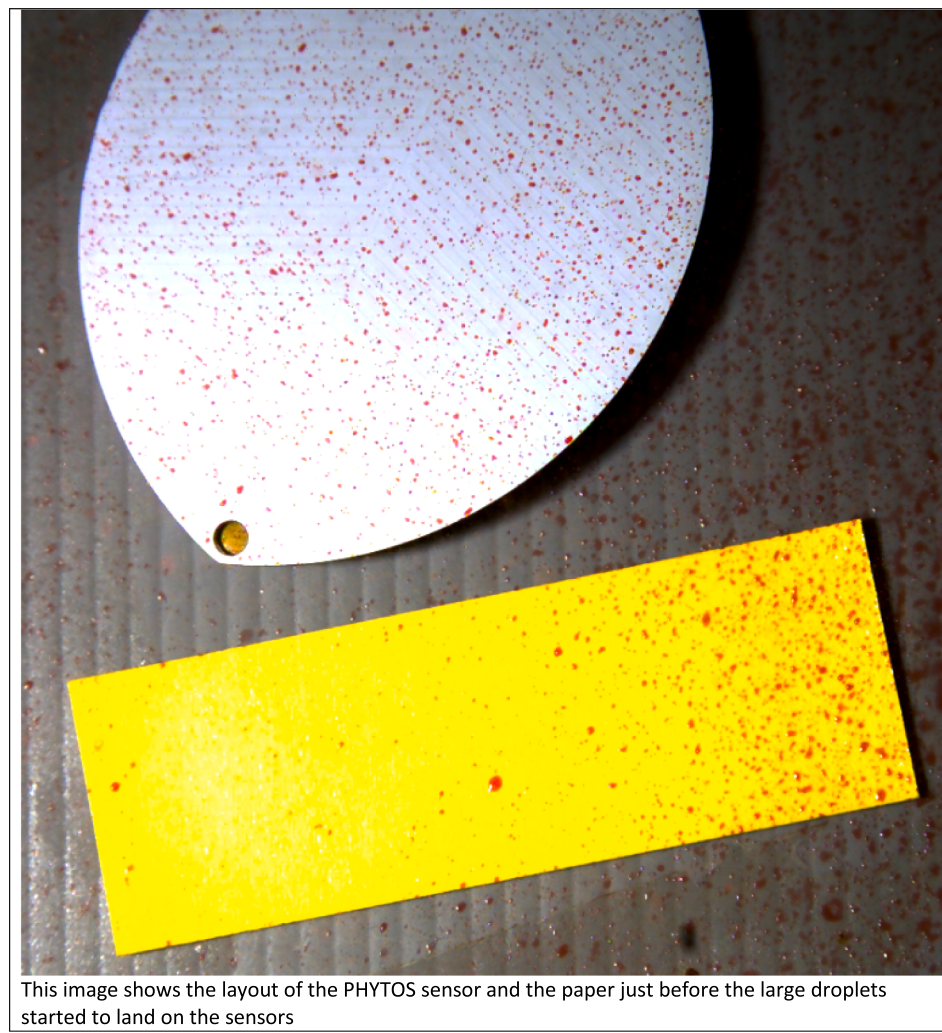


Fig. 10. Sequential frames of the sensors being sprayed with the BP1 nozzle.

(3.2–4.3%).

Although showing the same trend, the water sensitive papers and the capacitive sensors reported different quantitative results, with the sensors reporting a smaller areal coverage than the papers. In the high speed video, drops on the PHYTOS 31 sensors were seen to retract after reaching their maximum spread. This was not apparent on the water sensitive papers. This would explain the drops, after reaching equilibrium, occupying a smaller surface area on the PHYTOS 31 sensor. This may be caused by contact line pinning on the fibrous outer layer of the paper, absent on the smoother surface of the PHYTOS sensor. Additionally, more drops would be expected to run off the PHYTOS sensor, and not be included in the steady-state signal. The initial high coverage, followed by a reduction due to retraction, matches the spike and decay in sensor signal observed by (Hornero et al., 2017).

If a droplet of a given volume spreads twice the diameter on the paper as it does on the capacitive sensor, the area of the drop will be fourfold higher on the paper. A fourfold increase is consistent with the behaviour seen in the high and the difference between papers and sensors on the side of the trunk. Although the back-of-trunk values only show a 1- to 2-fold increase with charging, these droplets would likely be smaller, meaning that the scanning will likely underestimate the paper coverage.

In our experience, the retraction (de-wetting) behaviour of droplets on smooth plant leaves is closer to that on the PHYTOS 31 sensors than on the water sensitive papers. The PHYTOS 31 sensors better replicate

the spreading behaviour of leaves.

Regardless of the dependence of calibration function on droplet size, the sensors still stand to provide a unique benefit to farmers who rely on spraying operations, as well as to researchers working in this field. The ability to rapidly receive, process and display data with simple, easy to handle, and reusable equipment can speed up research drastically by removing the necessity for manual processing of water sensitive papers. It also can reduce the cost of disposables such as plastic bags, gloves, or tongs used to handle and store the papers in between testing and analysing. Farmers who just need to know whether all parts of their crop have been sprayed to a satisfactory level can use an array of these sensors throughout the canopy to measure where the dry parts are. Spraying professionals may use these sensors to ensure that their spray is an adequate level before continuing with the operation.

5. Conclusions

The capacitive wetness sensors tested are a reliable tool for measuring the proportion to which an area is wetted. They are repeatable, with a rise time of < 0.2 s and a variation of < 1% when measuring a constant signal. They fit two simple calibration functions that allow the user to judge the proportion of the surface covered, though the user must first know whether the coverage will be due to small droplets from a sprayer, or from large droplets such as rain. Additionally, this calibration does not produce results that agree quantitatively with water

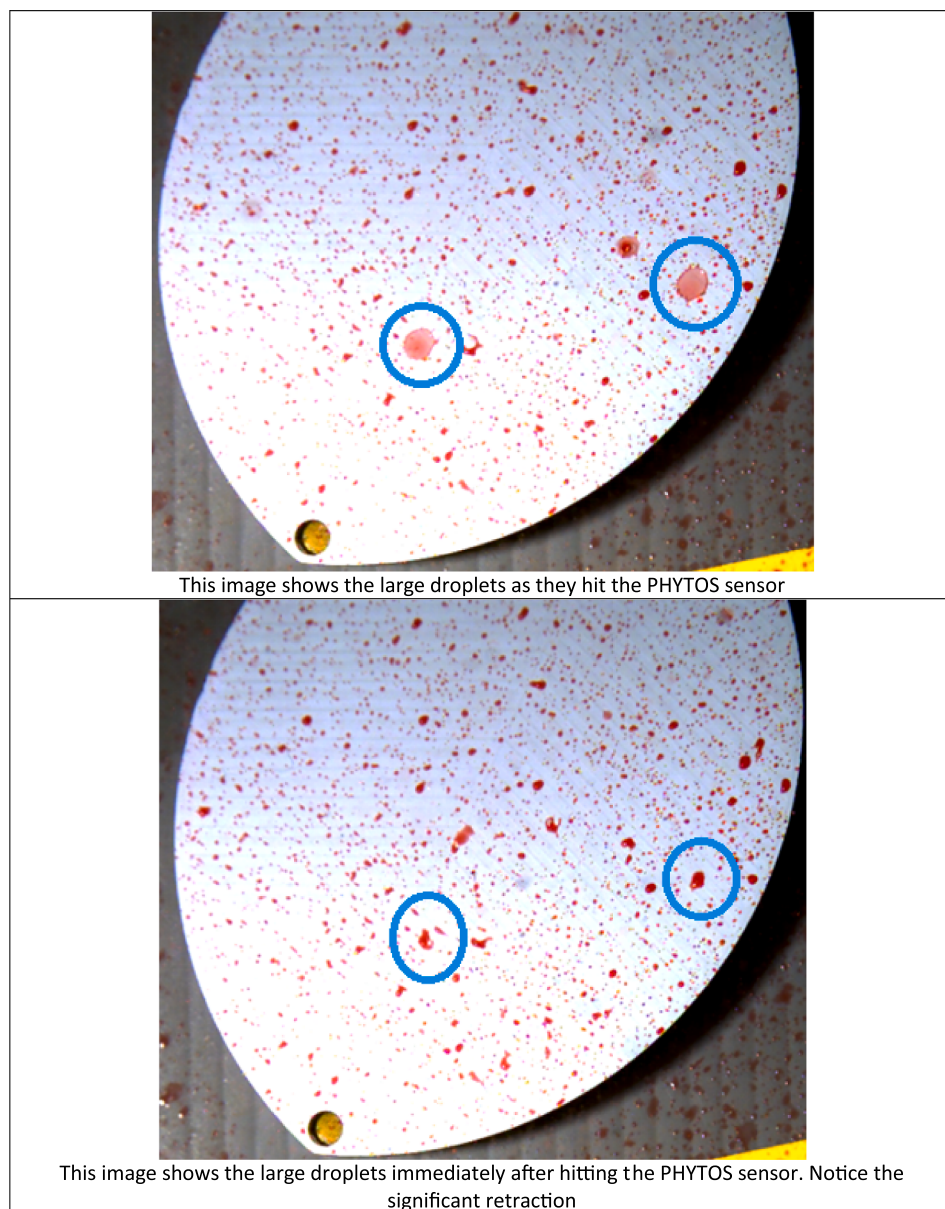


Fig. 10. (continued).

sensitive papers (though they do agree qualitatively), and further characterisation may prove useful for further research purposes. It is possible that the papers have always produced overestimates when compared to a hydrophobic leaf surface due to spreading with little retraction.

These sensors may provide a path for more accurate knowledge of spray coverage in regular spraying operations, allowing for a more delicate application process. This may lead to less wastage and pollution resulting from pesticide spraying. Researchers may use these sensors to provide much more prompt readings in experiments, improving efficiency.

CRediT authorship contribution statement

Luke Longworth: Conceptualization, Data curation, Formal

analysis, Investigation, Methodology, Writing- original draft, Writing: review and editing. **Scott Post:** Conceptualization, Methodology. **Mark Jermy:** Conceptualization, Methodology. **Hugh Hendrickson:** Investigation. **Jamie Steel:** Investigation. **Ethan Cannon:** Investigation. **Jack Gleadow:** Investigation. **Simon Brown:** Conceptualization, Methodology.

Declaration of Competing Interest

The authors declare that they have no known competing financial interests or personal relationships that could have appeared to influence the work reported in this paper.

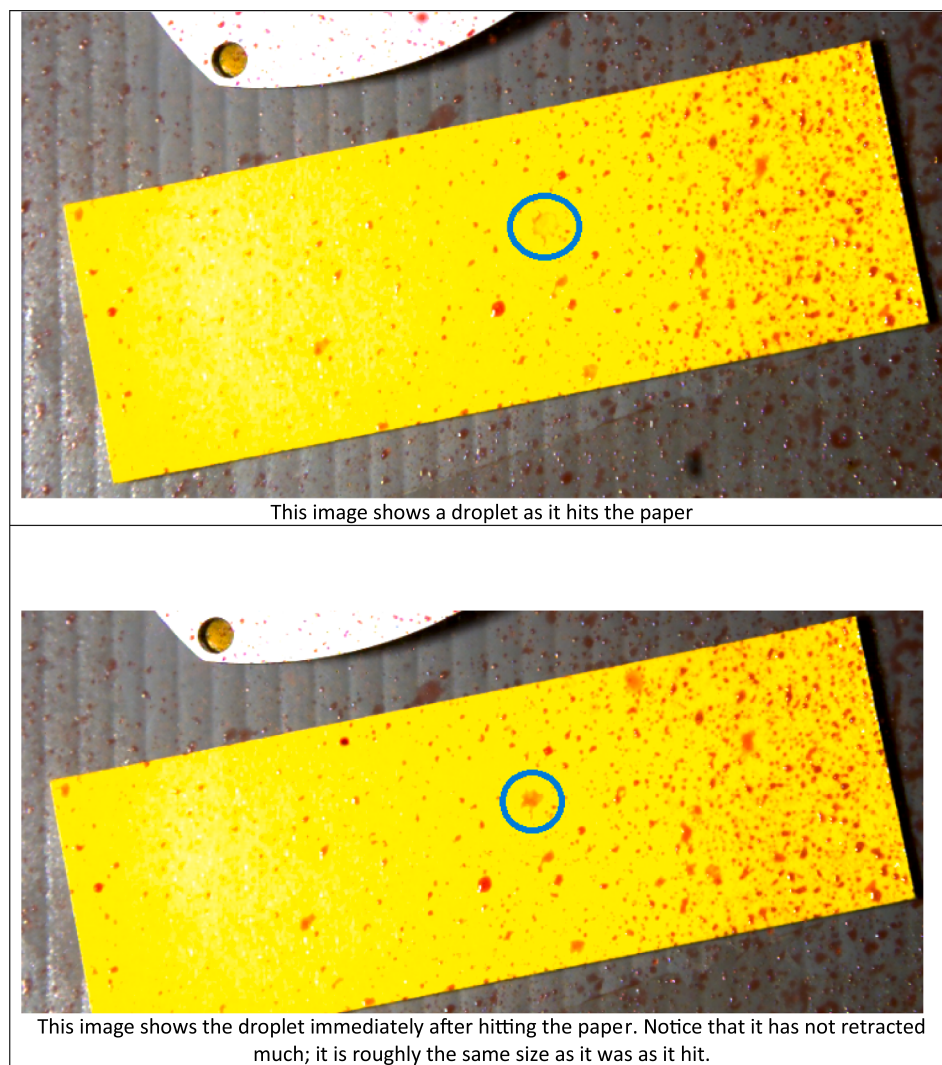


Fig. 10. (continued).

Appendix

The function was restricted to being non-negative, non-decreasing and concave up throughout the interval 0 to 1 (exclusive), and $y(0) = 0$. This section outlines the calculations that restrict a and b .

$$y = ax + (1 - a)x^b$$

$$y' = a + b(1 - a)x^{b-1}$$

$$y'' = b(b - 1)(1 - a)x^{b-2}$$

Rejection cases

- 1) For $b < 0$, $y(0)$ is undefined
- 2) For $b = 0$, curvature is zero everywhere
- 3) For $a = 1$, curvature is zero everywhere
- 4) For $b \in (0,1) \text{ & } a < 1$, curvature is negative
- 5) For $b \in (0,1) \text{ & } a > 1$, function is negative for $0 < x < \left(\frac{a}{a-1}\right)^{\frac{1}{b-1}} < 1$
- 6) For $b = 1$, curvature is zero everywhere
- 7) For $b > 1 \text{ & } a > 1$, curvature is negative
- 8) For $b > 1 \text{ & } a < 0$, function is negative for $0 < x < \left(\frac{a}{a-1}\right)^{\frac{1}{b-1}} < 1$
- 9) For $a = 0$, $y = x^b$, which is a simple power relationship and has been rejected already

Acceptance case

For $a \in (0,1)$, $b > 1$:

$$y(0) = 0^b = 0$$

$$y = x(a + (1 - a)x^{b-1}) > 0$$

For $x > 0$, this is true when $a + (1 - a)x^{b-1} > 0$

$$(a - 1)x^{b-1} < a$$

$$(a - 1) < 0, x^{b-1} > 0, a > 0$$

$$\therefore y > 0 \forall x \in (0, 1)$$

$$\dot{y} = a + b(1 - a)x^{b-1}$$

$$a > 0, b > 0, (1 - a) > 0, x^{b-1} > 0 \forall x \in (0, 1)$$

$$\therefore \dot{y} > 0 \forall x \in (0, 1)$$

$$\ddot{y} = b(b - 1)(1 - a)x^{b-2}$$

$$b > 0, (b - 1) > 0, (1 - a) > 0, x^{b-2} > 0 \forall x \in (0, 1)$$

$$\therefore \ddot{y} > 0 \forall x \in (0, 1)$$

Additionally, as b grows without bound, y approaches the linear case of $y = ax$ on the interval of 0–1. Because the data appears to deviate from a linear pattern around $x = 0.2$, high values of b are unlikely to be a good fit. Thus, b was searched over the interval of 1–10.

Appendix A. Supplementary material

Supplementary data to this article can be found online at <https://doi.org/10.1016/j.compag.2020.105829>.

References

- Acharya, B.S., Stebler, E., Zou, C.B., 2017. Monitoring litter interception of rainfall using leaf wetness sensor under controlled and field conditions. *Hydrol. Process.* 240–249.
- Australian Wine Research Institute Equipment adjustment and evaluation to maximise spray coverage [Online] // The Australian Wine Research Institute. - 2010. - 01 May 2019. - https://www.awri.com.au/wp-content/uploads/spray_equipment.pdf.
- Camuffo, D., della Valle, A., Becherini, F., 2018. A critical analysis of one standard and five methods to monitor surface wetness and time-of-wetness. *Theor. Appl. Climatol.* 1143–1151.
- Clark, S., 2018. Remote Monitoring of Cherry Wetness Using a Leaf Wetness Sensor and a Wireless Sensor Network [Book]. - New Orleans : University of New Orleans.
- Connor, Ferguson J., et al., 2016. Assessing the deposition and canopy penetration of nozzles with different spray qualities in an oat (*Avena sativa* L.) canopy. [s.l.]. *Crop Prot.* Vol. 81.
- Ehlert, K., et al., 2019. Comparison of wetness sensors and the development of a new sensor for apple scab prognosis. *J. Plant Dis. Prot.* 429–436.
- Foque, D., et al., 2018. Evaluating the usability of a leaf wetness sensor as a spray tech monitoring tool. *Aspects Appl. Biol.* 137, 191–200.
- Fox Robert, D., Derkson Richard, C., Braze Ross, D., 1998. Air-Blast/Air Assisted Application Equipment and Drift in: North American Conference on Pesticide Spray Drift Management. - Portland : [s.n.], pp. 108–129.
- Hornero, G., et al., 2017. A novel low-cost smart leaf wetness sensor. *Comput. Electron. Agric.* 43, 286–292.
- Kawahara, Y., Lee, H., Tentzeris, M.M., 2012. SenSprout: Inkjet-Printed Soil Moisture and Leaf Wetness Sensor. ACM Conference on Ubiquitous Computing. - Pittsburgh 545.
- Kesterson, M.A., Luck, J.D., Sama, M.P., 2015. Development and preliminary evaluation of a spray deposition sensing system for improving pesticide application. *Sensors* 31965–31972.
- Kesterson, M.A., Luck, J.D., Sama, M.P., 2015. Development and preliminary evaluation of a spray deposition sensing system for improving pesticide application. *Sensors* 31965–31972.
- Kesterson, M.A., Luck, J.D., Sama, M.P., 2015. Development and preliminary evaluation of a spray. *Sensors* 15, 31965–31972.
- Kishi Misa, et al., 1995. Relationship of pesticide spraying to signs and symptoms in Indonesian farmers. *Scand. J. Work Environ. Health* 21, 2.
- Law Edward, S., 2001. Agricultural electrostatic spray application: a review of significant research and development during the 20th century. *J. Electrostat.* 25–42.
- Longworth Luke, 2020. Effects of electrostatically charging pesticide sprays and quantitative methods for measuring spray efficacy [Report]. Masters thesis, University of Canterbury, New Zealand.
- Marlborough District Council, 2015. Rules relating to the application of agrichemicals [Online] // Marlborough District Council. July. https://www.marlborough.govt.nz/repository/libraries/id:1w1mps0ir17q9sgxanf9/hierarchy/Documents/Environment/Air%20Quality/Rules_for_Application_of_Agrichemicals.pdf.
- McEvoy Miles, 1998. Pesticide Drift and Organic Certification [Conference] // North American Conference on Pesticide Spray Drift Management. - Maine : University of Maine Cooperative Extension, the Land Grant University of the State of Maine and the United States Department of Agriculture, pp. 39–44.
- Meter Group Inc. Predicting the amount of water on the surface of the PHYTOS 31 dielectric leaf wetness sensor [Journal].
- Nazarko Orla, et al., 2002. Pesticide-Free Production (PFP). *Pestic. Outlook* 3.
- UN Food and Agriculture Organization, 2020. <http://www.fao.org/faostat/en/#search/Pesticides%20total>.
- Wang, P., et al., 2019. Monitoring of the pesticide droplet deposition with a novel capacitance sensor. *Switzerland : Sensors* 19, 537.
- Wen, Y., Zhang, R., Chen, L., 2019. A new spray deposition pattern measurement system based on spectral analysis of a fluorescent tracer. *Comput. Electron. Agric.* 14–22.
- World Health Organisation. Pesticide residues in food [Online] // World Health Organisation. - 19 February 2018. - <https://www.who.int/en/news-room/fact-sheets/detail/pesticide-residues-in-food>.
- Zhang Wenjun, 2018. Global pesticide use: Profile, trend, cost / benefit and more. [Book].